Supporting Information

Supplementary Data

Supplementary Table I.

	k_{cat} (s^{-1} x 10^{-2})	K_M (mM)	k_{cat}/K_M (s^{-1} mM^{-1} x 10^{-4})	Relative k_{cat}/K_M
WT	15.1 ± 0.6	7.2 ± 0.8	210.2 ± 25.6	1
G126	5.7 ± 0.1	25.9 ± 1.4	21.9 ± 1.3	0.1
ΔY125	6.5 ± 0.4	23.5 ± 2.9	27.6 ± 3.7	0.13

Kinetic parameters obtained for WT, G126, and ΔY125 PHPT1 through steady-state kinetics using pNPP as the substrate at 37˚C.

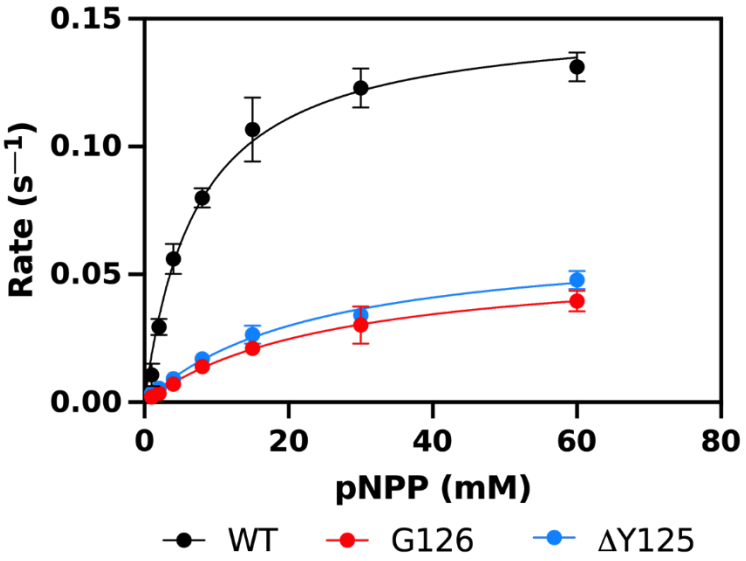

Supplementary Figure 1. Kinetic parameters obtained for WT, G126 and ΔY125 PHPT1 through steady-state kinetics using pNPP as the substrate at 37 ˚C.

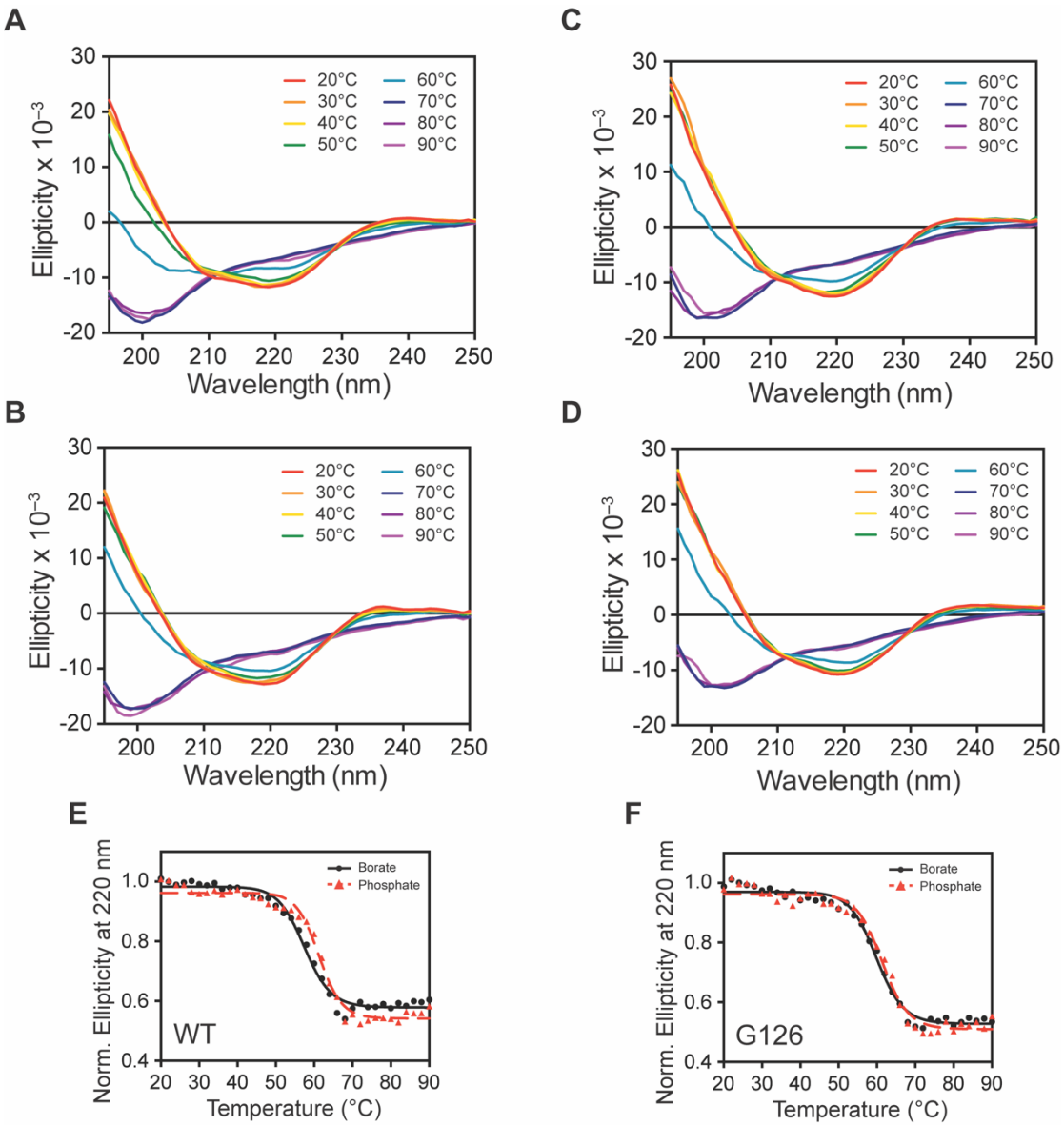

Supplementary Figure 2. CD spectra for WT (A and B), G126 (C and D) in borate (A and C) and phosphate (B and D) buffers. Spectra were collected every 2°C from 20°C to 90°C. Select CD spectra are shown from red to purple in 10 °C increments. (E and F) Molar ellipticity at 220 nm as a function of temperature for borate (black circles, solid lines) and phosphate buffer (red triangles, dashed lines) for (E) WT and (F) G126 PHPT1.

Supplementary Table II.

	Buffer Conditions	T_m (°C)
WT	5 mM borate, pH 9.0, 0.5 mM TCEP	57.4 ± 0.4
G126	5 mM borate, pH 9.0, 0.5 mM TCEP	59.9 ± 0.4
WT	5 mM Na_2HPO_4, pH 8.0, 0.5 mM TCEP	61.3 ± 0.4
G126	5 mM Na_2HPO_4, pH 8.0, 0.5 mM TCEP	61.4 ± 0.4

CD melting data. Obtained by fitting molar ellipticities at 220 nm at varying temperatures using equations 1 and 2 in the main text.

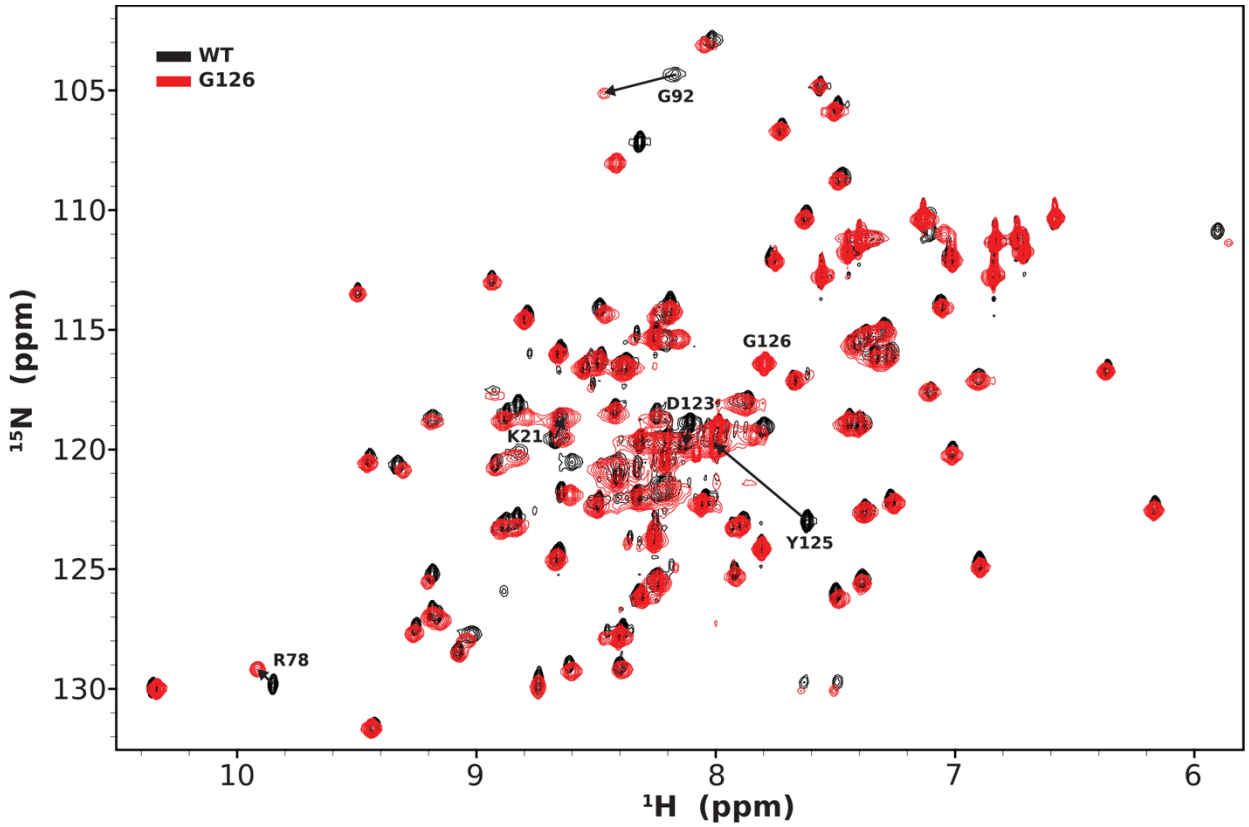

Supplementary Figure 3. ^{15}N-HSQC spectra of apo WT (black) and apo G126 (red) PHPT1. Residues K21, R78, G92, D123, and Y125 show CSPs above the significance cutoff.

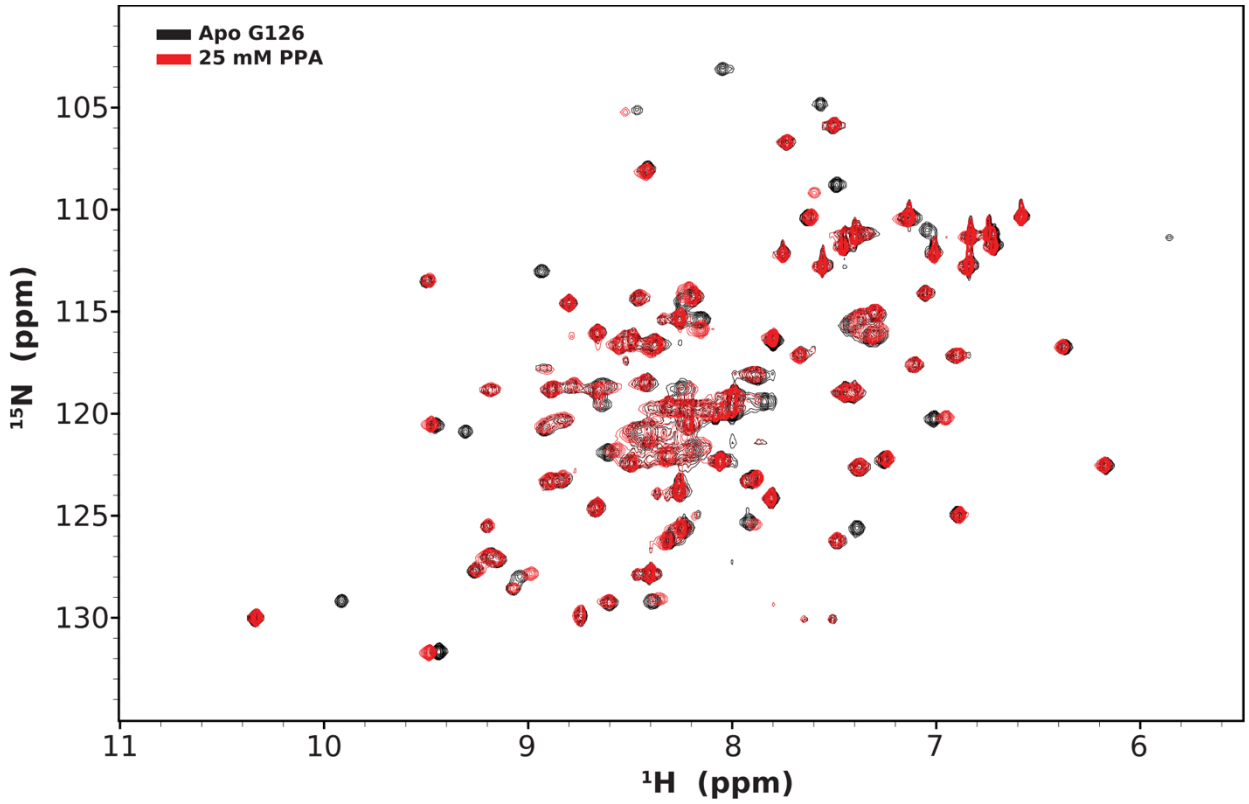

Supplementary Figure 4. ^{15}N-HSQC for G126 PHPT1 in presence (red) and absence (black) of 25 mM PPA.

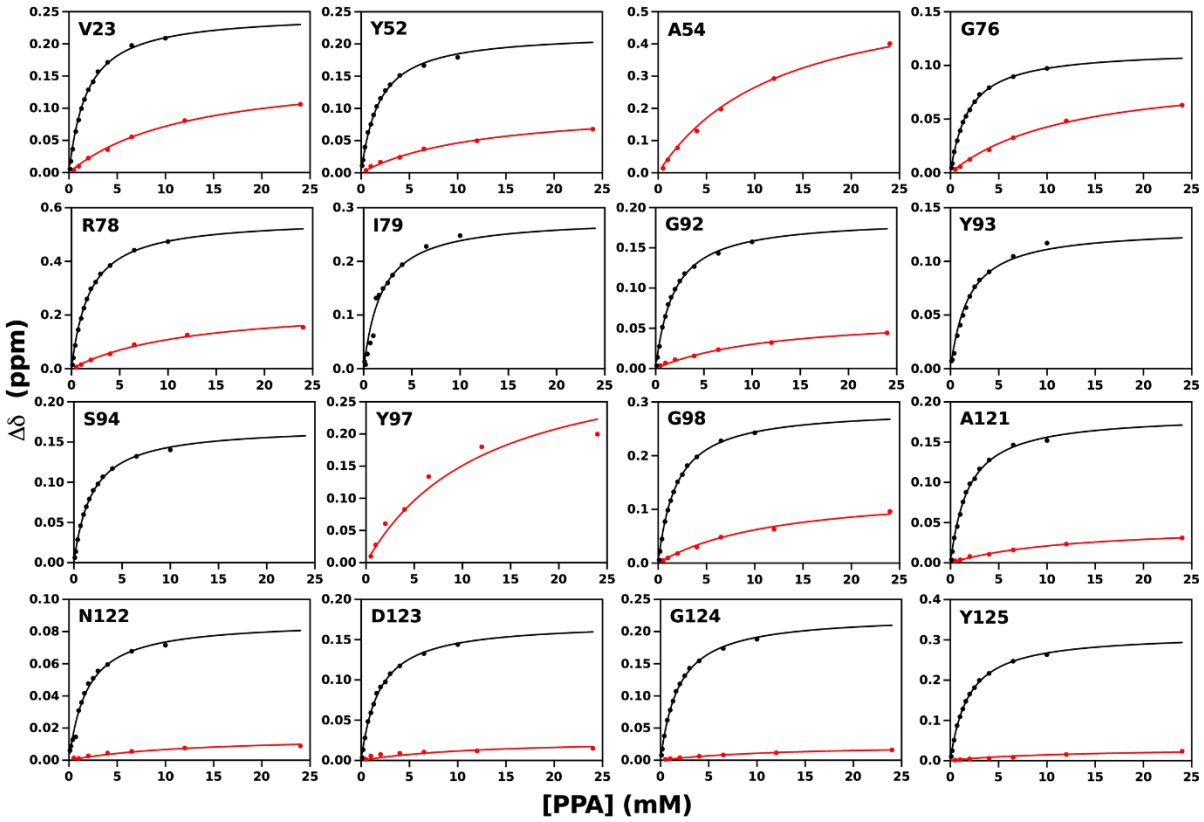

Supplementary Figure 5. Chemical shift titration analysis of residues exhibiting perturbations in the presence of PPA for WT (black) and G126 (red) PHPT1.

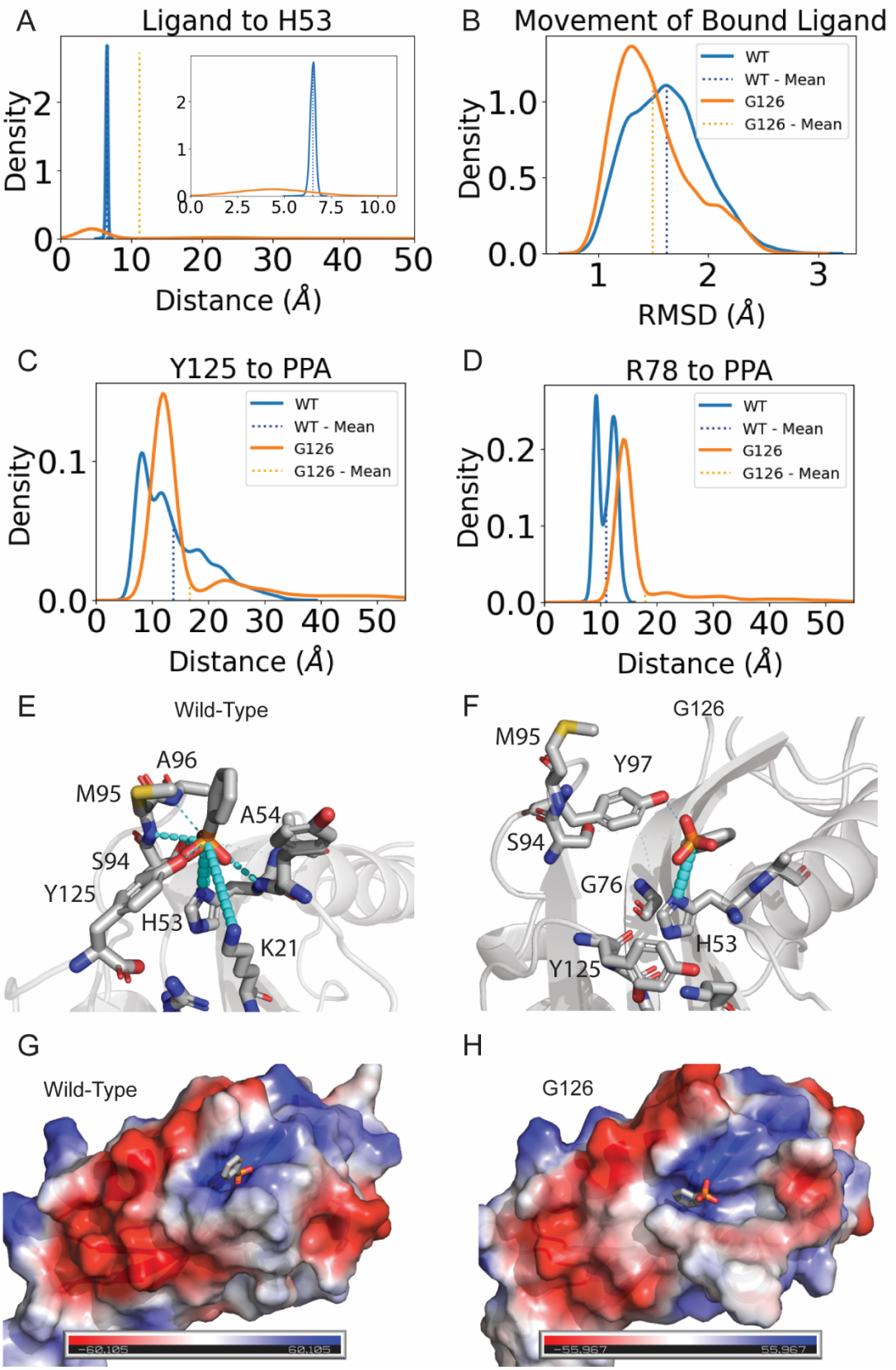

Supplementary Figure 6. PPA bound PHPT1. (A) Relevant distances between the center of masses of H53 and PPA as obtained from the simulated dynamics of WT (blue) and G126

(orange) PHPT1. WT shows a narrow distribution, suggesting large conservation of this distance unlike G126 which shows overall a broader distribution. The smaller distance of the ligand to H53 in the G126 data set is attributed to the altered orientation of bound PPA. In WT PHPT1, PPA sits above the imidazole of H53 and faces away from H53. In G126 PHPT1, PPA lies parallel to H53 decreasing the distance in the center of mass. The WT mean and mode were 6.52 and 6.57 Å, respectively. The G126 mean and mode were 11.1 and 4.42 Å, respectively. (B) Mobility of PPA in the active site pocket as measured by the ligand RMSD. The increased RMSD seen for WT PHPT1 is likely due to the ability of PPA to rotate in the active site, while the PPA in G126 undergoes translational movement, evidenced by the larger distribution of distances in (A). The WT mean and mode match with a value of 1.62 Å. The G126 mean and mode were 1.49 and 1.31 Å , respectively. (C) Distance distribution computed between the center of masses of residue Y125 and PPA as obtained from the simulated dynamics of WT and G126. The WT mean and mode were 13.79 and 8.16 Å, respectively. The G126 mean and mode were 16.63 and 11.91, respectively. (D) Distance distribution computed between the center of masses of the R78 guanidinium group and PPA as obtained from the simulated dynamics of WT and G126. The WT mean and mode were 11.02 and 9.24 Å, respectively. The G126 mean and mode were 17.87 and 14.07 Å, respectively. (E, F) Non-covalent polar (light blue) interactions between PPA and PHPT1 as computed from molecular dynamics simulations of WT and G126. Edge thickness is proportional to the interaction persistency. (G, H) Electrostatics protein surfaces (calculated in pymol) are shown for WT (G) and G126 (H) PHPT1 to show the differences in binding environment and PPA orientation.

Supplementary Table III.

Donor Amino Acid	WT Percentage (%)	G126 Percentage (%)
K21 - H1	-	-
K21 - H2	41.1	-
K21 - H3	36.7	-
H53 - H1	47.2	-
H53 - H2 - O1	95.0	45.5
H53 - H2 - O2	96.7	43.2
H53 - H2 - O3	98.3	18.1
A54	3.9	0.6
G76	-	0.9
R78 - H1	-	-
R78 - H2	-	-
S94	30.0	2.6
M95	50.6	0.1
A96	13.9	-
Y97	-	7.9
Y125	16.7	-
Total	**530.1**	**118.9**

Details of non-covalent polar interactions between PPA and PHPT1 as computed from molecular dynamics simulations of WT and G126. The percentage value is calculated by taking the number of frames where the interaction is present over the total number of frames in the trajectory. Averages for K21 and H53 in the WT data set are 38.9% and 84.3%, respectively. The average for H53 in the G126 data set is 35.6%.

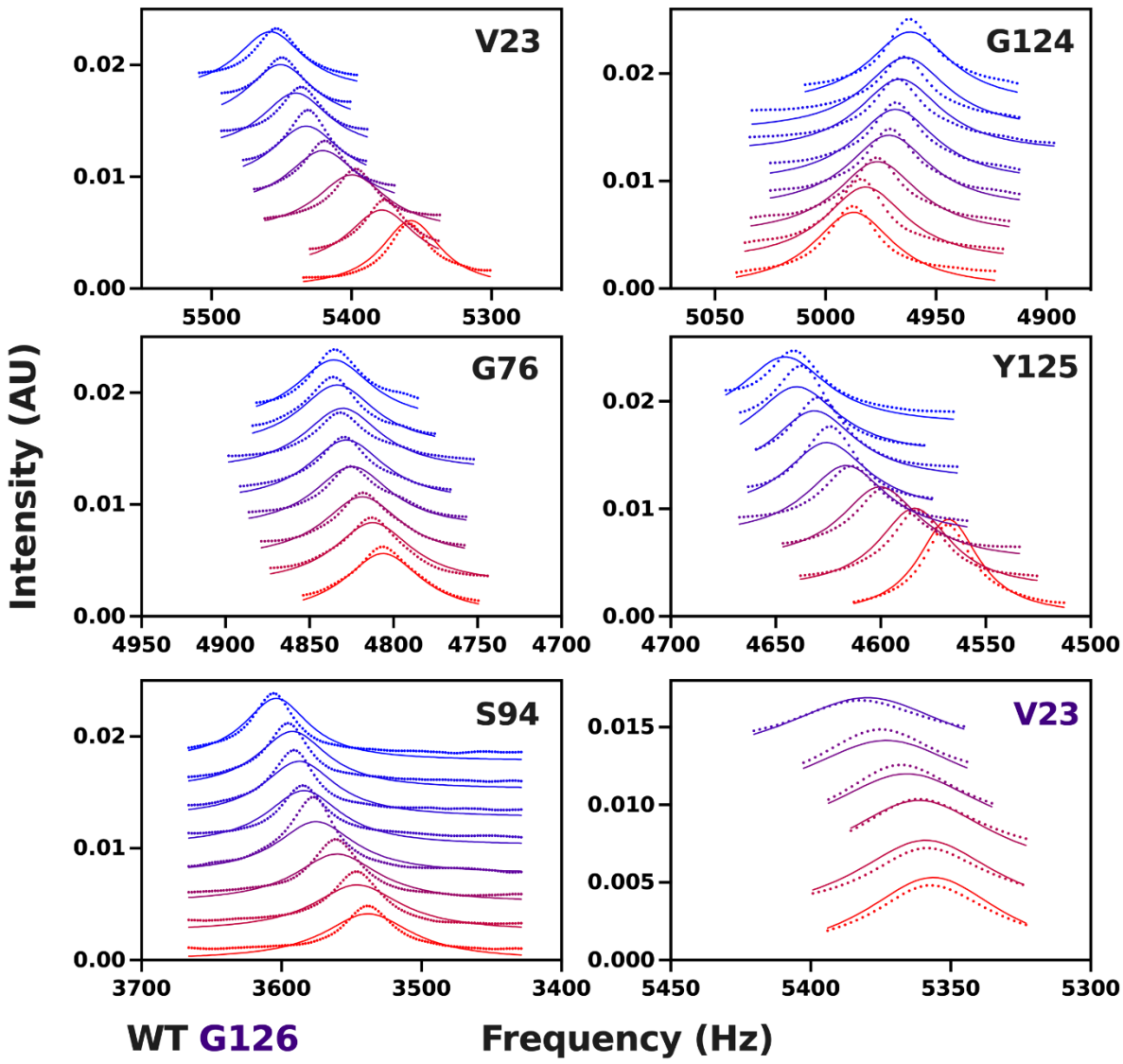

Supplementary Figure 7. PPA titration line shape analysis for the additional resonances used to obtain a global fit for binding kinetic parameters. Residues labeled in a black (purple) font belong to WT (G126) PHPT1.

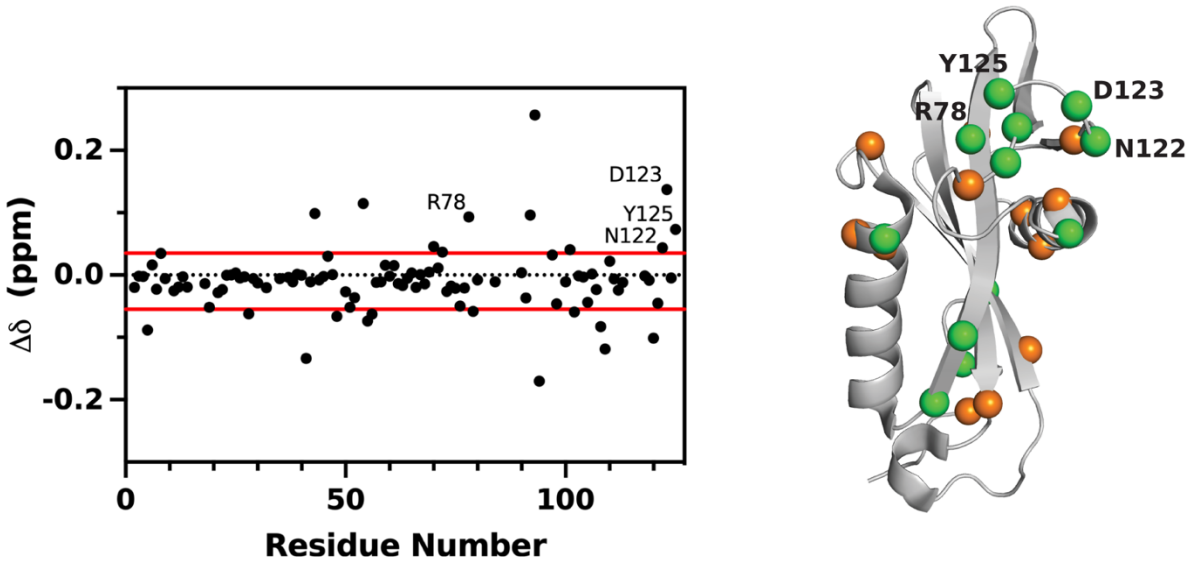

Supplementary Figure 8. NaCl effects on PHPT1. Differential CSP values are plotted against residue number. The CSPs in each enzyme upon adding salt (50 to 400 mM) were subtracted from each other (WT - G126). The red lines signify 1.5 times the standard deviation above and below the 10% trimmed mean. Positive (negative) values indicate a greater perturbation upon adding salt in WT (G126) PHPT1. Residues above and below the cutoff were mapped onto the PHPT1 structure (PDB: 2AI6). Spheres in green (orange) showed significant perturbations above (below) the cutoff.